Journal of Nuclear Materials 145–147 (1987) 453–457
North-Holland, Amsterdam

AN IN-SITU TECHNIQUE TO MEASURE EROSION AND DEPOSITION IN FUSION DEVICES

David N. RUZIC and Glenn A. GERDIN

Department of Nuclear Engineering, University of Illinois, Urbana, IL 61801, USA

Key words: erosion rate, limiter/divertor plates, carbon, wall erosion, erosion probe measurements

Erosion or deposition of sub-micron layers of graphite or other materials can be measured by bombarding a sub-surface layer of ^{10}B or ^{6}Li with thermal neutrons and observing with a surface-barrier detector the energy loss of the prompt alphas or tritons produced. To demonstrate the feasibility of this technique, a (5250 ± 250) Å layer of boron and a (1.25 ± 0.05) μm layer of $Li_2B_4O_7$ were electron-beam evaporated onto graphite substrates and exposed to a thermal neutron flux of $(8.0 \pm 0.5) \times 10^5$ cm^{-2} s^{-1}. The (n,α) reactions of the ^{10}B produce a 1.78 MeV α, a 1.48 MeV α, and a 0.848 MeV ^{7}Li. The reactions of ^{6}Li produce a 2.73 MeV ^{3}H and a 2.05 MeV α. Carbon coatings of (600 ± 25) Å, (8250 ± 500) Å, (2.0 ± 0.2) μm, and (4.0 ± 0.4) μm were placed between the active layers and a surface barrier detector in vacuuo. The thinner layers shifted the 1.48 MeV α peak by (31.7 ± 4.5) keV and (431 ± 43) keV respectively. The thicker layers shifted the 2.73 MeV ^{3}H peak by (206 ± 15) keV and (346 ± 20) keV respectfully. Therefore, utilizing boron implants, 100 Å to 1 μm of graphite erosion or redeposition can be determined. Utilizing lithium implants, thicknesses in the range of 1 μm to 10 μm can be determined. Theoretical energy shifts, thermal diffusion, and the feasibility of this technique as a between shot diagnostic for limiters, divertor plates, and/or first-wall armor are discussed.

1. Introduction

The particle fluxes of future magnetic confinement devices may be high enough to critically damage limiters, divertor plates and/or first-wall components through erosion in a short period of time. Erosion rates on the order of 10 cm/y have been estimated for their graphite limiters and walls [1]. Redeposition of C may greatly reduce the effect [2], but quantitative details of this process remain largely unknown [3]. Indeed, sputtering of the limiter/divertor is generally considered as a primary feasibility problem for future machines [4].

Direct measurement of erosion and redeposition have been made by several groups [5–10], but these were performed by removing structures that had been exposed to many discharges. During that time a variety of plasmas heating schemes, disruptions and other events may occur. Time and discharge resolved erosion/deposition measurements have been obtained by implanting ^{13}C into ASDEX probes [11], but the probe itself may melt or influence the erosion/deposition, and the sample still has to be analyzed. In-situ measurements have been performed by activating a thin surface layer and monitoring the change in the number of gammas produced [12], but the layer had a relatively short (16 day) half-life and little lateral sensitivity was possible. The diagnostic proposed in this paper can measure erosion and deposition in the range of 100 Å to μm in-situ and between plasma discharges on any preselected surface reachable by a small (2 cm^3) surface barrier detector. In this procedure no high-Z or radioactive material is introduced into the discharge.

Certain limiter, divertor plate and/or first wall graphite tiles would be prepared with the inclusion of a thin (approximately 0.5 μm) layer of a ^{10}B and/or ^{6}Li containing compound 0.1 to 10 μm below the surface. (See fig. 1.) Between discharges, a thermal neutron source, such as a commercially available D–T well-logger with its tip surrounded by a 45 cm radius polyethylene sphere, placed on the outside of the vacuum vessel would be turned on and a surface barrier detector on the end of a probe would be inserted into the vessel over the implanted layer. The energy spectra of the alpha particles and tritons produced from the (n, α) reactions would be shifted by an amount dependent on

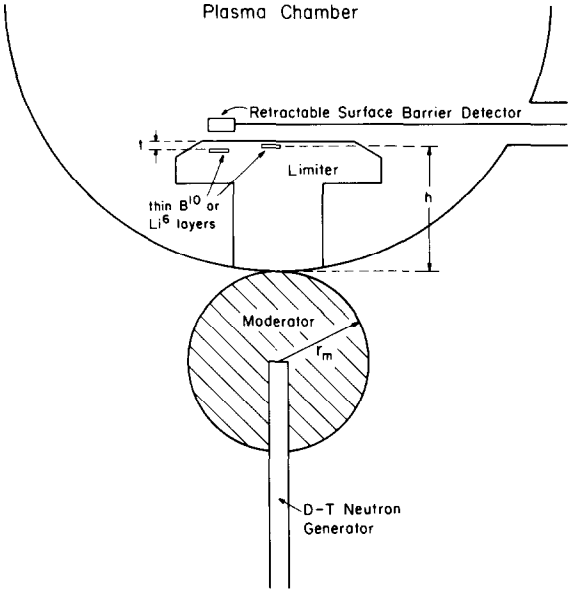

Fig. 1. Schematic of proposed in-situ between shot erosion/deposition diagnostic.

the thickness of the intervening material. Calibration could be continually checked using the same probe by irradiating an implanted layer external to the fusion device. The following sections describe the results of a proof-of-principle experiment and discuss the feasibility of implementing this diagnostic technique.

2. Experimental

Polycrystalline boron, and in a separate run, powdered lithium tetraborate ($Li_2B_4O_7$), were electron-beam evaporated out of a carbon crucible onto 1 cm^2 polished graphite and single crystal silicon wafers. To obtain a sharp step parts of the silicon substrates were masked by silicon chips. Using that step, the thickness of the layers were determined to be (5250 ± 250) Å for the boron and (1.25 ± 0.05) μm for the $Li_2B_4O_7$. The uniformity of the deposition was within the uncertainty of the thickness measurement. Auger analysis showed about 50% carbon contamination in the boron deposit and no contamination in the $Li_2B_4O_7$. Some of the samples were then coated with (600 ± 25) Å, or (8250 ± 500) Å of evaporated carbon. No contamination of these over-layers was detected.

Individually, the samples were placed in a rough-pumped vacuum chamber 5 mm from an Ortec 4.0 cm^2 surface barrier detector and exposed to a thermal neutron flux of $(8.0 \pm 0.5) \times 10^5$ cm^{-2} s^{-1} from the University of Illinois TRIGA nuclear reactor.

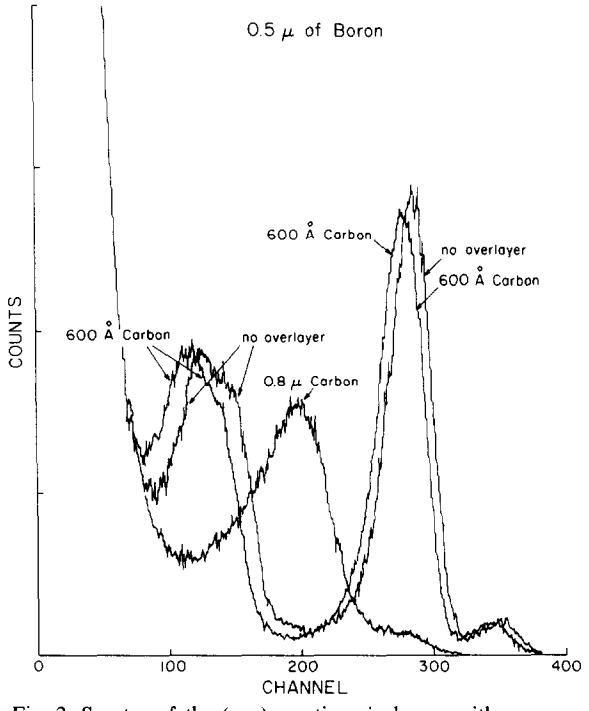

Fig. 2. Spectra of the (n,α) reactions in boron with no overlayer, a 600 Å overlayer of carbon, and a 0.825 μm layer of carbon. For the unshifted spectra the 1.78 MeV α peak occurs near the channel 350, the main 1.48 MeV α occurs near channel 290 and the 0.848 MeV ^{7}Li near the channel 150.

The (n, α) reactions of the ^{10}B produce a 1.78 MeV α, a 1.48 MeV α, and a 0.848 MeV ^{7}Li ion. The 1.48 MeV α is due to an excited state in the Li nucleus and is the dominant peak occurring 94% of the time [13]. The reactions of ^{6}Li produce a 2.73 MeV ^{3}H, and a 2.05 MeV α. The ^{3}H peak and an ^{235}U check source were used to calibrate the 1024-channel analyzer at (5.035 ± 0.037) keV per channel. The 0-channel offset was negligible.

Fig. 2 shows the spectra from the boron coatings. As expected, the carbon layers shift the ^{7}Li energy more than the alpha's. In fact, for the thicker layer, the ^{7}Li peak is shifted completely into the noise. Experimental energy shifts were determined by smoothing the data and measuring the shift between the midpoints of the high energy edge of the peaks. This technique minimizes the effect of straggling through the boron layer itself. Results are shown in table 1.

Fig. 3 shows the spectra from the $Li_2B_4O_7$ irradiations. As expected, the triton peak shifts very little compared to the alpha and ^{7}Li peaks. The 1.48 MeV α peak is much broader on the low energy side than in fig. 2 because the active layer is 2.4 times thicker. Once again, the ^{7}Li peak is shifted into the noise for the 0.825 μm C coating. The energy shifts for the alpha and ^{7}Li are extracted the same way and are also in table 1.

To measure larger triton shifts, (2.0 ± 0.2) μm and (4.0 ± 0.4) μm carbon foils from Lebow Foil Corporation were inserted between the ^{6}Li-containing sample and the detector. The sample to detector distance was now 9 mm. This worsened the count rate due to a decreased solid angle, but provided much larger shifts. Fig. 4 shows an expanded view of the triton peak for all 5 cases. The upper half of these curves show little asymmetry and were fitted to a Gaussian to extract the position of the peaks [14]. That data also appears in table 1.

Material structures in fusion devices are often sub-

Table 1
Experimental and calculated energy shifts in keV for the major peaks in figs. 2–4

	Experiment	Calculation
2.73 MeV ^{3}H		
600 Å	23.2 ± 1.4	5.9 ± 1.2
8250 Å	94.2 ± 1.9	79 ± 16
2 μm	206 ± 16	173 ± 35
4 μm	346 ± 30	343.0 ± 69
1.48 MeV α		
600 Å	31.7 ± 4.5	33 ± 6.6
8250 Å	431 ± 43	488 ± 86
0.848 MeV ^{7}Li		
600 Å	49.4 ± 2.0	54 ± 11

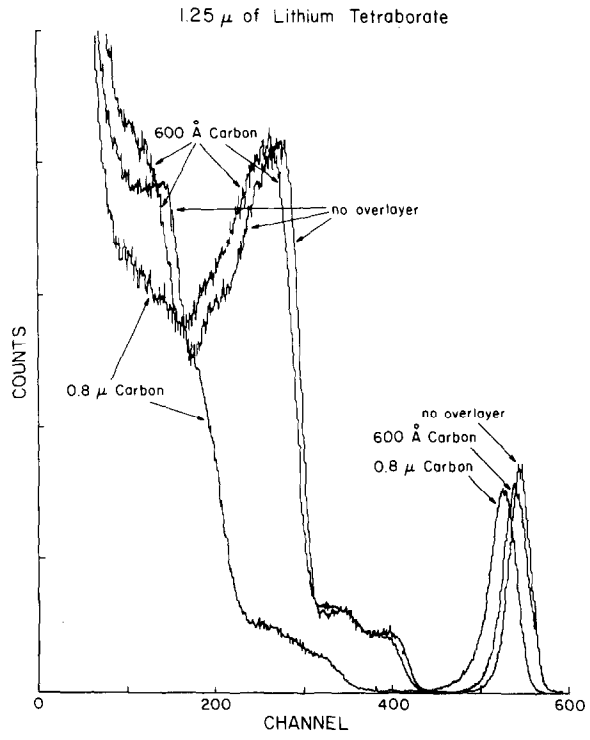

Fig. 3. Spectra of the (n,α) reactions in $Li_2B_4O_7$ with no overlayer, a 600 Å overlayer of carbon, and a 0.825 μm layer of carbon. For the unshifted spectra the 2.73 MeV ^3H peak occurs near channel 550, the 2.05 MeV α near channel 400, and the rest of the peaks as in fig. 2.

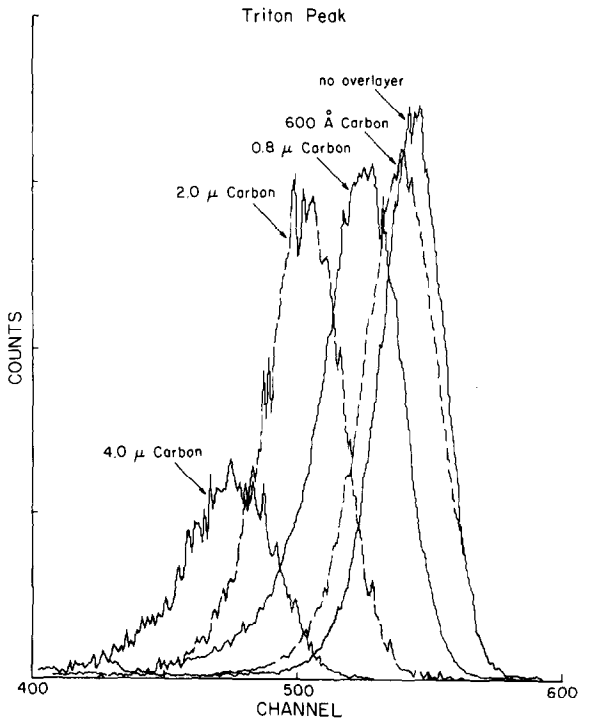

Fig. 4. Expanded view of the triton peak shifts for 4 overlayer thicknesses. The no overlayer and first two thicknesses have the same number of total counts. The 2 μm and 4 μm cases had fewer counts and have been expanded by a factor of 5.

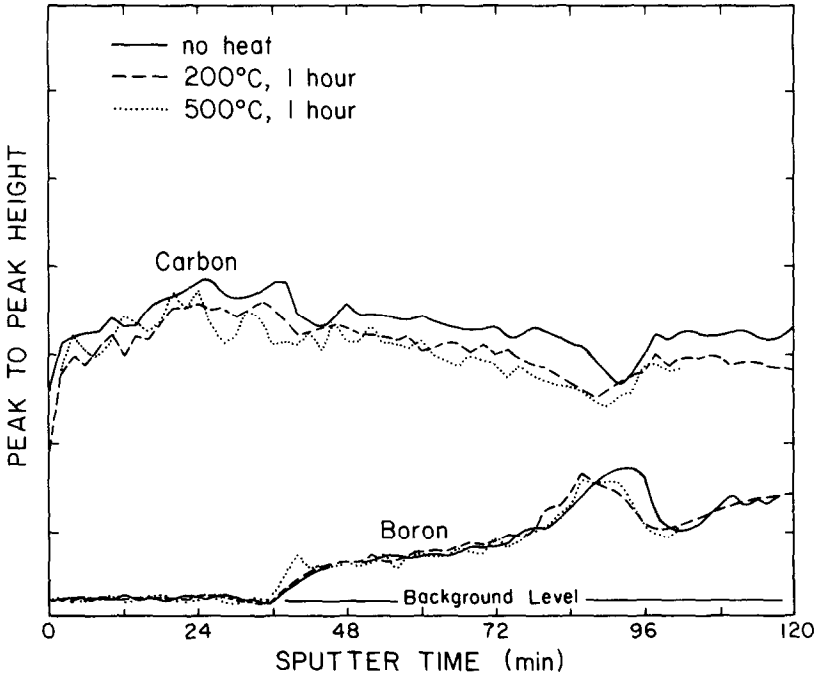

Fig. 5. Auger depth profiles of boron–carbon samples coated with 600 Å of carbon after differing heat treatments. In all three cases the boron became detectable only after 36 min of sputtering. The composition of the evaporated material varied during the deposition process as exemplified by the peak in the boron concentration at 90 min.

ject to thermal shock and high temperatures. If the active layer thermally diffused into the bulk, this diagnostic would fail. To test thermal diffusion, identical samples with 600 Å of carbon overlaying the boron–carbon layer were vacuum baked. One sample was held at 200°C for 1 h; the other was held at 500°C for 1 h. Auger depth profiles were performed on each and on an un-baked sample. As seen in fig. 5, the profiles were virtually identical indicating no thermal diffusion at these moderate temperatures. An earlier sample was baked at 1700°C for 15 min, but became contaminated in the oven. Though the degree of diffusion (if any) is uncertain, a boron layer was still evident indicating that total diffusion did not occur.

3. Theory

Theoreticial energy shifts obtained from birth energies, tabulated curves [15–17] of dE/dx, and the coating thickness would underestimate the experimental shift by nearly a factor of two. One reason is a finite source thickness. The energetic particles born farthest from the detector must pass through the active layer as well as the coating. This broadens the peak and slightly increases the shift since the slope of $dE/dx(E)$ is negative. However, this effect is at most 16% (for T through the 1.2 μm $Li_2B_4O_7$). The major factor increasing the energy shift and broadening the peak is the solid angle. The energetic particle spectra from the (n, α) reaction is angularly isotropic. Since the detector had almost a 2π solid angle and 4 times greater area than the area of the source, many of the energetic particles traveled obliquely through the active layer and coating before reaching the source. Integration over the possible paths showed that the average distance traveled through the carbon overlayer was 1.48 times t, where t is the thickness of the overlayer. For the inserted carbon foils this enhancement factor was 1.29. The theoretical energy shifts, corrected for solid angle and self shielding by the source are shown in table 1. The errors associated with these values are due to uncertainties in dE/dx.

In a diagnostic application, allowing oblique flight paths permits the 100 Å depth resolution demonstrated in this experiment. Lateral resolution equals the width of the detector or implanted layer, whichever is smaller. The solid angle could be reduced through collimation thus increasing lateral resolution, but would decrease the count rate prohibitively.

The count rate is limited by the thermal neutron flux available to the sample. A cylindrically shaped 14.1 MeV D–T neutron generator 2.54 m long with a 4.3 cm OD produces 10^8 neutrons per second [18]. Those neutrons must be moderated to thermal energies. Polyethylene is the obvious choice for a moderator since it is solid, easy to fabricate, and behaves like H_2O in hydrogen content and density. To estimate the amount of polyethylene required we used age-diffusion theory [19] for the slowing down of 14.1 MeV neutrons in water. The slowing down length has been calculated [20] to be 13 cm, corresponding to a Fermi age radius of 32 cm for a point source of fast neutrons in an infinite moderator. At 32 cm the thermal neutron flux, ϕ, is 0.22 times that of the peak thermal neutron flux in the center, $\phi(0)$. To come closer to approximating an infinite medium, the design radius, r_m, has been increased to 45 cm. At this distance $\phi = 0.05\ \phi(0)$.

Table 2
Expected count rates in counts/min for a 0.5 μm thick 1 cm^2 layer of natural B, pure ^{10}B, natural Li, and pure ^{6}Li for varying distances away from the vessel wall. (See fig. 1.) A source strength of 10^8 D–T neutrons/s and a 45 cm radius polyethylene moderator are assumed

h	Nat. B	^{10}B	Nat. Li	^{6}Li
10 cm	415	2100	13	175
20 cm	295	1500	9	125
30 cm	225	1150	7	95
50 cm	140	700	4	60

The cross-section for the ^{6}Li(n,α)^{3}H and ^{10}B(n,α)^{7}Li reactions are 945 b and 3813 b respectively for thermal neutrons. Natural Li is 7.5% ^{6}Li and natural boron is 19.8% ^{10}B. Table 2 shows the counts/min expected from a 0.5 μm thick 1 cm^2 layer of natural B, pure ^{10}B, natural Li, and pure ^{6}Li as a function of h, the distance from the edge of the polyethylene to the active layer.

4. Discussion

Since this diagnostic requires moveable probes and boron or lithium sub-surface implants, erosion or deposition can only be measured at pre-selected locations. Prime candidates are limiters and divertor plates themselves as well as the device walls close to these structures. The count rates in table 2, particularly if pure ^{10}B is used, are high enough to enable the detection of as little as 100 Å of carbon erosion or deposition at these locations by counting for 10 min. A boron layer would give the thicknesses of layers up to 1 μm. To gauge thicker changes, the tritons from ^{6}Li could be measured. Limited detector resolution is probably responsible for the larger-than-expected triton energy shift through the 600 Å coating shown in table 1. To avoid these small shifts, the usuable range for the tritons is 0.5 μm to 10 μm. The lateral spatial resolution for all the cases is 0.5 cm. Non-uniform erosion over that distance would widen the peaks but an average erosion would still be calculable.

Some additional advantages of this diagnostic include the usefulness of a small compact 14.1 MeV source for calibrating the response of other diagnostics, and the use of Li or B. Should the implanted layers be completely eroded away, low-Z non-radioactive material

is introduced to the plasma. Future work will include testing the thermal diffusion and fabrication properties of various Li and B containing compounds, and experimentally verifying the moderation properties of polyethylene in a realistic geometry.

We wish to thank Mr Howard Savage and Mr Bruce Cain for helping produce the coatings at the Construction Engineering Research Laboratory, Dr Nancy Finnegan for helping with the Auger analysis at the UIUC Materials Research Laboratory, and Professor Bernard W. Wehring of North Carolina State University for advice on the thermal neutron calculations. This work has been supported in part by a National Science Foundation Presidential Young Investigator grant awarded to one of the authors (D.N.R.).

References

[1] D. Heifetz, D. Post, M. Ulrickson and J. Schmidt, J. Nucl. Mater. 111 & 112 (1982) 298.
[2] J.N. Brooks and M. Kaminsky, Fusion Technol. 6 (1984) 465.
[3] Folker Engelman, in: Physics of Plasma–Wall Interactions in Controlled Fusion, NATO ASI Series B: Physics, Vol. 131, Eds. D.E. Post and R. Behrisch (Plenum Press, New York, 1986) p.32.
[4] Technical Assessement of the Critical Issues and Problem Areas in the Plasma Materials Interaction Field, Vol. 1, PPG-765, Eds. R.W. Conn, W.B. Gauster, D. Heifetz, E. Marmar and K.L. Wilson (Center for Plasma Physics and Fusion Engineering UCLA, Los Angeles, 1984) C-16.
[5] S.A. Cohen, R. Budney, G.M. McCracken and M. Ulrickson, Nucl. Fusion 21 (1981) 233.
[6] TFR Group, J. Nucl. Mater. 128 & 129 (1984) 292.
[7] R. Behrisch, P. Børgesen, J. Ehrenberg, B.M.U. Scherzer, B.D. Sawicka and J.A. Sawicki, J. Nucl. Mater. 128 & 129 (1984) 470.
[8] Y. Hirohata, M. Mohri, T. Yamashina, P.W. Trester, G.R. Hopkins and T. Hino, J. Nucl. Mater. 128 & 129 (1984) 477.
[9] E. Franconi, M. Barteri and G.M. Ingo, J. Nucl. Mater. 128 & 129 (1984) 481.
[10] A.E. Pontau et al., J. Vac. Sci. A4 (1986) 1193.
[11] J.B. Roberto, J. Roth, E. Tauglauer and D.W. Holland, J. Nucl. Mater. 128 & 129 (1984) 244.
[12] D.H.J. Goodall, T.W. Conlon, C. Sofield and G.M. McCracken, J. Nucl. Mater. 76 & 77 (1978) 492.
[13] H. Bischel and T.W. Bonner, Phys. Rev. 108 (1957) 1052.
[14] Glenn F. Knoll, Radiation Detection and Measurement (John Wiley and Sons, New York, 1979) p. 738.
[15] H.H. Anderson and J.F. Ziegler, Hydrogen Stopping Powers and Ranges in All Elements, Vol. 3 of Stopping and Ranges of Ions in Matter (Pergamon Press, New York, 1977).
[16] J.F. Ziegler, Helium Stopping Powers and Ranges in All Elements, Vol. 4 of Stopping and Ranges of Ions in Matter (Pergamon Press, New York, 1977).
[17] J.F. Ziegler, Stopping Cross-Sections for Energetic Ions in All Elements, Vol. 5 of Stopping and Ranges of Ions in Matter (Pergamon Press, New York, 1980).
[18] Gene Swinerton, EMR Photoelectric Nuclear Corporation, Princeton NJ, private communication.
[19] J.J. Duderstadt and L.J. Hamilton, Nuclear Reactor Analysis (Wiley, New York, 1976) p. 367.
[20] H. Volkin, J. Appl. Phys. 26 (1955) 127.